Anthropogenic Impact in the Maya Lowlands of Petén, Guatemala

D. Battistel[*,a,b], M. Roman[a,c] , A. Marchetti [a,] , N. M. Kehrwald[b,d] , M. Radaelli [a,], E. Balliana[a], C. Barbante[a,b]

[a] Department of Environmental Science, Informatics and Statistics, University Ca' Foscari of Venice, Via Torino 155, 30170 Mestre Venezia, Venice, Italy.

[b]Institute for the Dynamics of Environmental Processes – CNR, University Ca' Foscari of Venice, Via Torino 155, 30170 Mestre Venezia, Venice, Italy.

[c] ECSIN-European Center for the Sustainable Impact of Nanotechnology, ECAMRICERT SRL, Viale Porta Adige 45, 45100 Rovigo, Italy

[d] U.S. Geological Survey, Geosciences and Environmental Change Science Center, Denver, CO 80225, USA

* Corresponding author e-mail: dario.battistel@unive.it

Keywords: Petén Itzá, Trace Element, Rare Earth Element, Maya Civilization, Sedimentary Records.

Abstract

Trace and rare earth elements were determined in a sedimentary core (PI 5 VI 02 11B) collected from lake Peten Itzá (Guatemala). Several diagnostic element ratios and principal component analysis were used to depict the geochemical dynamics that affected the lake since ~5500 y BP. This time period covers the Preclassic and Classic (from ~3000 to ~900 y BP), where Mayan societies thrived, contributing to forest loss and land clearance for agriculture. We demonstrated that variations in precipitation and agricultural practices altered land-use and associated erosional processes in the basin. Indeed, low to high rare earth element ratios (LREE/HREE) showed high precipitation rates between 3 to 1 ky BP, also correlating to an increase in allocthonous silicates input into the lake and low organic carbon content in correspondence of the Maya Clay layer. The geochemical composition of lake sediments, combined with palynological records, indicated a re-growth of the tropical forest after ~900 y BP, coincident with the decline of large-scale Mayan agriculture as a consequence of a severe drought amplified by the anthropogenic land-use.

The analysis of As and Hg sequence showed that anomalous spikes, corresponding to several documented volcanic eruptions, were likely due to natural atmospheric inputs rather than anthropogenic. Moreover, the enrichment factors calculated for platinum and iridium showed that the concentration of these elements were ~50 and ~400 times higher than Earth's crust average. Although similar PGEs data are not available for the surrounding lakes, these enrichments may be a legacy of the asteroid impact that formed Chicxulub crater ~65 My ago.

Introduction

The ancient Maya impacted the tropical forests of Mesoamerica (Vaughan et al. 1985, Islebe et al. 1996, Leyden et al. 2002) to such a degree that Beach et al., (2015) coined the term *Mayacene* (Maya Early Anthropocene) to denote the environmental changes resulting from prehistoric Mayan activities. In the Yucatán Peninsula (Mexico) and Guatemala (Binford, 1987), Mayan societies thrived between ~3000 to ~900 y BP, creating complex infrastructures such as temples, wetland fields, canals, terraces and field ridges (Gill et al. 2000, Peterson and Haug 2005). Agriculture was their main source of livelihood, where maize (*Zea mays*) contributed at least to the 70% of their diet (Diamond, 2000 and references therein). During the Early and Mid-Preclassic periods (from ~3500 to ~2300 y BP), the early rural population typically used slash-and-burn agricultural practices, contributing to forest loss and land clearance, as supported by charcoal and levoglucosan records (Schüpbach et al. 2015). Slush-and-burn agriculture, however, is not suitable for sustaining large populations, as the exploited soil needs several decades in order to naturally recover its original fertility (Kotto-Same et al. 1997). When Mayan population peaked at 13 million people, during the Classic period (1750-1100 y BP) (Peterson and Haug 2005), with an estimated population density of 100-300 individuals per km^2 (Rice and Rice, 1990; Curtis et al. 1998, Brenner 1983), the exponential demographic growth required developing new agricultural techniques. This agricultural expansion resulted in where terraces, canal networks and irrigation systems ensured a more efficient agricultural production (Scarborough 1993, Beach et al. 2002; Gill 2000; Beach et al. 2009; Luzzadder-Beach 2009). Although their advanced agricultural system was likely able to bear possible long droughts, Mayan societies abruptly collapsed ~900 y BP (Curtis et al. 1996; Whitmore et al. 1996; Haug et al. 2003; Kennet et al 2012).

Anthropologists and natural scientists investigate the demise of the Mayan civilization due to the many analogies between the Late Classic and modern times, as a warning for possible future scenarios. Several authors interpret the Maya collapse as an exclusive consequence of their agricultural and building activities that led to forest decline and soil erosion, while recent studies propose that environmental changes occurring in the Lowlands were primarily forced by climate change (Hodell et al. 2000; Brenner et al. 2002; Mueller et al 2009). However, these climate changes may have been triggered by anthropogenic factors as land-use and forest clearance could have acted as positive feedbacks for droughts by increasing albedo and decreasing evapo-transpiration, thus limiting the annual rainfall (Rosenmeier et al. 2002).

Palaeo-environmental proxy records, such as pollen (Wahl et al. 2006), oxygen (Curtis et al. 1998; Mueller et al. 2009) and carbon isotopes (Beach et al. 2011), as well as monosaccharide anhydrides and charcoal (Schüpbach et al. 2015) obtained from environmental archives collected in the Lowlands infer the Maya impact on the landscape. The Lowlands were an essential center of the Mayan civilization and Lake Petén Itzá (Guatemala), in particular, located ~25 km from the flourishing center of Tikal, is a promising palaeo-environmental archive. Previous studies demonstrated that Petén Itzá lake levels are mainly controlled by the evaporation : precipitation (E:P) balance and the lake did not desiccate during long dry periods (Curtis et al. 1998; Hillesheim et al. 2005; Anselmetti et al. 2006; Hodell et al. 2008; Correa-Metrio et al. 2012). The relatively high sedimentation rate ranging from 270 mm 1000 y^{-1} in the period before ~4 ky BP to 1140 mm 1000 y^{-1} during the Preclassic, (Mueller et al. 2009, Hillesheim et al. 2005, Schupbach et al. 2015), provides a temporal resolution between ~10 and ~40 y cm^{-1}, which is suitable for investigating the development and decline of the Mayan civilization.

Although soil erosion during the Preclassic and Classic periods is well-evidenced by the Maya Clay stratigraphic section (Curtis et al. 1998; Anselmetti et al. 2007; Mueller et al. 2009), multi-elemental sequences of trace (TE) and rare earth elements (REE) provide additional insights that help decipher the anthropogenic impact and the Classic Maya collapse dynamics. To the best of our knowledge, TE (i.e. Cu, Fe, Mn, Pb, Zn, Au and Hg) (Beach et al. 1998; Dahlin et al. 2007, Eberl et al. 2012; Huston and Terry, 2006; Luzzadder-Beach et al, 2011; Middleton, 2004, Parnell

et al. 2002, Wells et al. 2000) and REE (Cook et al., 2006; Beach et al. 2006; Beach et al. 2008) have been determined only in soil and sediment samples from north-western Yucatán to south-western Guatemala, but a high resolution record that encompasses the Mid-Late Holocene in the Petén region is not yet available.

Here, we provide high resolution records of trace and rare earth elements in a sedimentary core collected from Lake Petén Itzá, spanning the last ~5500 years. Diagnostic element ratios and principal component analyses depict the geochemical dynamics that affected the lake since the Mid-Holocene. These elemental records provide an innovative way of examining the Mayan civilization expansion and collapse with respect to with climatic and environmental factors.

Study site

Lake Petén Itzá (17°00'N, 89°50'W) **(Fig.1)**, located at ~ 110 m a.s.l. in the Central Petén Lake District of northern Guatemala, is the deepest lake of the Mayan Lowlands with a maximum depth of ~165 m. Its surface area is ~ 100 km^2 and lake waters are dominated by high concentration of calcium (63 mg l^{-1}) , magnesium (23 mg l^{-1}), sulfate (101 mg l^{-1}) and bicarbonate (198 mg l^{-1}) that provide high pH values (pH ~ 8) (Hillesheim et al 2005).

Precipitation varies seasonally based on the seasonal migration of the Inter-tropical Convergence Zone (ITCZ) and the Azores-Bermuda high pressure system (Deevey et al. 1980; Hodell et al. 2008). The rainy season (from June to October) is characterized by precipitation between 900 and 2500 mm y^{-1} (Deevey et al. 1980). However, when the ITCZ and Azores-Bermuda high-pressure systems move southward (January to May), strong trade winds dominate and precipitation decreases, leading to a pronounced dry season. The Lake Petén Itzá basin is fed mainly by precipitation and subsurface ground-water inflow, where other external inputs are limited to a small stream in the southeast (Correa-Metrio et al. 2012, Hillesheim et al. 2005).

Materials and Methods

Samples and Age Model

Six piston cores were collected in Lake Petén Itzá in June 2002 using a Kullenberg piston corer triggered by a mud-water interface corer (Anselmetti et al. 2007, Hillesheim et al. 2005). In this work we used the 550 cm long PI 5 VI 02 11B core that covers the Holocene. The 55 samples were sub-sampled from the original core at the University of Florida, USA, and shipped to the University of Venice in 2012. The samples were frieze-dried, grinded using a ball mill, homogenized and stored at -20°C until analysis. The sediment core for the section with a depth from 18 to 300 cm was subsampled into 2.5-cm samples taken every 5 cm, while the core section with a depth of 300 cm to 355 cm was subsampled into 1-cm samples taken every 2 cm.

In this paper we used the same age model reported in Schüpbach et al.(2015), that was obtained using a total of 12 radiocarbon dates from this same core and a parallel core (11A) reported in Mueller et al. (2009) and Hillesheim et al. (2005). This age model results in an age span from ~150 to ~5300 yr BP for the PI 5 VI 02 11 B core section between 18 and 355 cm.

Analytical Methods

Elemental analyses were performed on aliquots of 0.5 g of freeze-dried and homogenized sediment. Sample digestions were performed using a microwave assisted digestion system (Milestone® Ethos1 + Milestone® HPR-1000/10S High Pressure), following a two-step procedure. In the first step, each sample was treated with a solution containing 2 mL HNO_3 + 6 mL HCl ultrapure acids (ROMIL) in order to maximize the extraction efficiency of the ultra-trace elements (Pt, Ir and Au). The temperature program was 10 min of ramp-up time and 5 min of hold time at a temperature of 160 °C, followed by 15 min of ramp-up time and 45 min of hold time at a temperature of 230 °C. After centrifuging at 1000 rpm for 5 minutes, the liquid fraction (I) was separated from the solid residue. During the second step, the residues were treated with 2 mL HF

Suprapure + 6 mL HNO_3 ultrapure acids (ROMIL), thus obtaining a second fraction (II). All digested fractions (I and II) were diluted with ultra-pure water (ELGA LabWater, Marlow, UK) to a final volume of 40 mL.

Fractions I and II were further diluted (1:100) and separately analyzed using an Inductively Coupled Plasma – Quadrupole Mass Spectrometer (ICP-MS, model 7500cx from Agilent Technologies) equipped with autosampler (ASX-500 Cetac technologies) and operating both in standard and collision mode (He flux 4 mL min^{-1}). The quantitative analysis of platinum group elements (PGEs) Pt and Ir, plus Au, was performed in an independent run. Elements quantification was carried out by external calibration using multi-elemental standards (IV-STOCK-6 for Ag, Al, As, Bi, Cd, Co, Cr, Cu, Fe, Mn, Mo, Ni, Pb, Sr, U, V, and Zn; IV-STOCK-26 for Rare Earth elements; MSHG-10PPM for Hg; IV-STOCK-28 for Sn and Sb; all standards were purchased from Inorganic Ventures). The concentration of each element was obtained by pooling the values from fractions I and II.

Eight replicates of the certified estuarine sediment (BCR-667) and 10 procedural blanks were processed and analyzed like the samples throughout the study for method validation. The analytical performances are reported in **Table 1S,** as Supporting Material. The method limit of detection (LOD_{met}) for each element was calculated as the mean plus three times the standard deviation of procedural blanks. The apparent recoveries for BCR-667 ranged between 89 and 111 % (except for As (130 %), Au (81 %) and U (114 %)), The intermediate precision expressed as relative standard deviation (RSD), was below 8% for the majority of the elements considered. It must be noted, however, that the higher RSD values obtained for Ir (15%) and Pt (12%), were due to their low concentrations in BCR-667 samples (Ir = 0.9 ± 0.1 ng g^{-1} and Pt =3.0 ± 0.4 ng g^{-1}).

Total inorganic carbon (TIC) was also determined in the same samples using a TOC 5050 Analyzer (Shimadzu), following the procedure described in Wang et al. (2012). Briefly, 20 mg of dried sediment were treated with 0.5 mL of acid aqueous solution (H_3PO_4/ water 1/1 v/v) and CO_2 produced by carbonates decomposition at 200°C was measured in duplicate by Fourier transform infrared spectroscopy. Na_2CO_3 standard (0.3, 0.75 and 1 mgC) and blank solutions were used for external calibration.

Statistics and Data Analysis

Principal component analysis (PCA) was performed to obtain correlations between variables and to infer possible processes that control elemental distribution. The concentration of all elements analyzed, total organic carbon (TOC%, from Schüpbach et al. (2015), obtained in the same record), TIC, sedimentation rate, and elemental ratios that can be associated with environmental redox conditions (i.e. V/(V+Ni) (Hatch and Leventhal, 1992; Gao et al. 2014), Fe/Mn (Wersin et al. 1991) and V/Cr (Jones and Manning, 1994)) were used as the input variables for PCA. Normality of data distribution was assessed using the Shapiro-Wilk test (Shapiro and Wilk, 1965; Royston et al. 1992) at a 95% confidence level. W-coefficient and *p*-values are reported in **Table 1**. The majority of elemental concentrations were normally distributed. Non-normal elemental distributions were log-transformed. The dataset was then transformed into z-scores prior to PCA analysis. Only eigenvalues larger than 1 were considered, according to the Kaiser-Gutmann criterion. Varimax rotation was also applied to minimize the number of variables with high loadings on each principal component.

Enrichment factors (EFs) for each element (i) were calculated using the simplest form proposed by Reimann and De Caritat (20009:

$$EF(i) = \frac{[Al]_{ref}}{[Al]_{sample}} \frac{[i]_{sample}}{[i]_{ref}}$$

(1)

where [i] is the average concentration in the sample of the i-th element, the subscript *ref* indicates the use of Earth's crust (Rudnick and Gao, 2014) or shale (Average Shale (Tribovillard et al. 2006, Taylor et al. 2010) or Northern American Shale Composite (NASC) (Haskin et al. 1966; Gromet et al. 1984)) as reference. Aluminum concentrations were used as the conservative element for normalization (Reimann and De Caritat, 2000).

Results

Distribution and variability of elements in Lake Petén Itzá

Trace and Rare Earth Element concentrations were determined in 55 samples along the sediment core section. REE concentrations were reported as a sum (ΣREEs*), except for cerium that was considered separately (REE will be discussed in more detail in the following paragraphs). As reported in **Table 1**, Al and Fe are the most abundant trace elements (average 48.9 and 21.4 mg g^{-1}, respectively) and the majority of the elemental concentrations did not markedly differ from those reported for Earth's crustal average (Rudnick and Gao, 2014). Only Ir and Pt showed values significantly higher than the certified estuarine sediment (3-10 and 8-29 ng g^{-1}, respectively) and the Earth's crustal average for the whole dataset. Several elements, such as Co, Ni, V, U, Pb and Sr did not vary significantly along the dataset (max/min ratios were close to 2), while Au and Sn, in particular, showed a higher variability (max/min ratios were 13.1 and 6.8, respectively, also associated with higher standard deviation, SD). However, Au concentrations were very close to the LOD_{met}. Furthermore the higher variability of Au may derive from the situation that microscopic specks of metallic Au are sometimes present in sediments, thereby hindering homogenization.

Principal Component Analysis

Principal Component Analysis is a useful tool to bring out the processes controlling elemental changes throughout the sedimentary record. Preliminary elaborationd showed that all REEs (except Ce), were very highly correlated to each other (r=0.96-0.99). We therefore performed a PCA using ΣREEs* as a single variable and considering Ce independently.

Table 2 reports the loadings of the variables from the PCA. The first four components explained 87.8% of the total variance. The first component explained 63.5% of the variance and is characterized by high positive loadings of lithophile elements such as Al(0.848), Cr(0.865), ΣREEs (0.788), and Fe(0.847), and by higher negative loadings of Sr (-0.690) and TIC (-0.816). The second component accounted for 15.1% of the total variance and is characterized by high positive loadings of Mo (0.861) and TOC (0.935), and negative loadings of the sedimentation rate (-0.899). The third component (5.2% of total variance) showed high positive loadings for the redox diagnostic indexes Fe/Mn (0.617) and V/(V+Ni) (0.718) and negative loadings for Mn (-0.725). The fourth component (4.0% of the total variance) showed high loadings of Pt (0.804), Ir (0.747) and Au (0.747).

The temporal evolution of each component is reported in **Fig. 2**. As is evident, PC1 and PC2 showed similar behaviors between 5.5 and ~3 ky BP. However, while PC2 continued to decrease, reaching minimum values between ~3 and ~1 ky BP, PC1 abruptly increased beginning around ~3 ky BP. After 1 ky BP, both PC1 and PC2 began to increase. Differently from PC1 and PC2, PC3 was quite stable between 5.5 and ~1 ky BP, but decreased in correspondence to the increase of PC1 and PC2, after ~1 ky BP. PC4 did not show any particular long-term trend, and was instead characterized by several spikes throughout the record.

Enrichment Factors

As is evident from **Table 3**, the majority of trace elements showed EF values very close to unity with no significant differences, for either Earth's crust or shale (Average Shale or NASC). However, when EFs (crustal) do significantly differ from EFs (shale), the enrichment values obtained were below or close to ~10, suggesting that the enrichments were only minor (Reimann and De Caritat, 2000). On the contrary, Ir and Pt had notably high EFs (386 and 50, respectively).

The temporal profiles of several enrichments, such as Hg and As are shown in **Fig.3**. Although the EFs of these elements were not particularly high, the records showed several anomalous peaks. In particular, EF(Hg) showed one peak at ~2250 y BP, while As showed two distinct peaks at ~1330 and ~2500 y BP, respectively. EF(Hg) at ~2250 y BP ($EF(Hg)^{2250}$=3.46) may be considered an outlier as EF $(Hg)^{2250}$ exceeds the background mean (mean=1.72) by more than three times the standard deviation (SD=0.31). Similarly, $EF(As)^{1330}$ and $EF(As)^{2500}$ (4.21 and 4.73, respectively) exceed the mean (mean=2.39) more than three times the standard deviation (SD=0.30). These outliers may be representative of punctual events, due to inputs enriched in Hg and/or As, that may be atmospherically transported into the basin.

Rare Earth Elements

The minimum and maximum REEs concentrations, in addition to the mean and the corresponding SD, were reported in **Table 4**. The ΣREE (Ce included) ranged from 56 to 133 μg g^{-1}, showing concentrations similar to those obtained in other lakes, such as Lake Rhino (China) (24-103 μg g^{-1}) (Wen et al 2014), Lake Baikal (Russia) (65-240 μg g^{-1}) (Och et al 2014) and Lake Acigög (Turkey) (9-99 μg g^{-1}) (Budakoglu et al. 2015).

The cerium anomaly (Ce/Ce*) was calculated as follows (Ederfield and Graves, 1982):

$$Ce/Ce^* = \frac{3Ce_N}{2La_N + Nd_N} \quad (2)$$

where N indicates the NASC-normalized concentration (Gromet et al. 1984). As shown in **Fig. 4**, Ce anomalies are very close to unity from 5.5 to ~ 3 ky BP, decreasing after 3 ky BP and reaching minimum values between ~2.5 and ~1 ky BP. After ~1 ky BP, Ce/Ce* increased again up to 0.95.
Cerium anomalies are due to the selective fractionation of this element with respect to the other REEs. While all the other REEs (except Eu) commonly display the only 3+ oxidation state in nature, Ce can exist as both trivalent (Ce^{3+}) and tetravalent (Ce^{4+}) forms (Xiong et al. 2012). In more oxidizing environments, Ce^{3+} is oxidized to Ce^{4+} and is then rapidly complexed by organic or inorganic ligands. Ce^{4+}-complexes are less soluble than their corresponding Ce^{3+}-complexes and thus precipitate preferentially, thereby enriching the sediment in Ce and depleting the water body. As shown in **Fig.4**, Cerium anomalies were always below unity, indicating that this mechanism can only partially explain the observed behavior. Moreover, both Ce^{3+} and Ce^{4+}-complexes are less soluble than the other REE-complexes. Leaching processes can also lead to REE fractionation as more soluble REE-complexes are preferentially transported into the lake, resulting in a net Ce-depletion in the sediment. In addition, Ce/Ce* can also be affected by other factors, such as diagenetic alterations, low/high water table and pore water-sediment exchange (Xiong et al. 2012, Murray et al. 1991, Hosler 1997, Kidder et al 2003). Thus, Ce/Ce* anomalies must be carefully examined when used as a paleoproxy.

The redox indexes V/(V+Ni) (Hatch and Leventhal, 1992; Gao et al. 2014), Fe/Mn (Wersin et al. 1991) and V/Cr (Jones and Manning, 1994) proposed in this paper poorly correlate with Ce/Ce* (V/(V+Ni) (r=-0.14; *p*-value=0.31), Fe/Mn (r=0.38; *p*-value=0.004) and V/Cr (r=0.46, *p*-value=0.049)), while correlating well with TOC% (r=0.79 *p*-value < 0.001) and the sedimentation rate (r=-0.87; p-value<0.001).

Due to the peculiar geochemistry of Ce described above, the element was not included in the following calculation of the low-to-high REEs ratio (LREE/HREE):

$$LREE/HREE = \frac{4(La_N + \mathrm{Pr}_N + Nd_N)}{3(Er_N + Tm_N + Yb_N + Lu_N)} \quad (3)$$

In sedimentary materials, LREEs commonly exhibit slightly higher concentration than HREEs (Aide and Aide 2012). The temporal profile of LREE/HREE, reported in **Fig. 4** is enriched in LREE between 5.5 and ~3 ky BP and after ~1 ky BP. However, in alkaline environments encriched in carbonates, HREEs are depleted in the authigenic sediments as HREE-carbonate complexes are preferentially distributed in the water fraction (Cantrell and Byrne, 1987; Lee and Byrne 1993). HREEs and LREEs can also undergo fractionation processes. In fact, HREE-complexes (and carbonates, in particular) show higher solubility than their corresponding LREE species (Luo and Byrne, 2004). Thus, preferential HREE leaching tends to decrease LREE/HREE ratio in the lake sediment. In Lake Petén Itzá sediments, LREE/HREE and carbonates (TIC) significantly correlate (r=0.68, *p*-value < 0.001) (see also **Fig. 4**), suggesting a possible predominance of *in situ* precipitation dynamics. Therefore, *ex-situ* preferential leaching or other possible mechanisms involving organic matter content and reactivity, or anthropogenic disturbances may be less important than the processes occurring within the lake (Pourret et al. 2007; Aide and Aide 2012).

Discussion

The first principal component positively correlates with lithophile elements (e.g. Al, Fe, Cr and REE) and likely represents the lithic fraction of the sediment. Aluminum, in particular, is not affected by biogenic or neogenic processes, such as *in situ* transformation along the water column or post-depositional processes in the sediment. Aluminum may therefore be reasonably indicative of the relative abundance of the allocthonous silicate fraction in the sediment. The negative correlation with TIC and Sr suggests that authigenic carbonate material may have accumulated in the sediment. This increase of carbonates with the decrease in the allocthonous silicate fraction may be have driven by a change in the E:P balance. Low lake levels may favor the precipitation of carbonates while, conversely, high precipitation may increase the contribution of the allocthonous fraction to the sediment. This interpretation is also consistent with the precipitation increase between ~3000 and ~1 ky BP observed in the neighboring Lake Salpetén $\delta^{18}O$ record (Rosenmeier et al 2002: **Fig.2)**, and the regional wet and warm conditions before ~4.5 ky BP (Mueller et al. 2009). PC1 thus encompasses these lake level processes, that were primarily driven by the E:P balance (Rosenmeier et al 2002) and is supported by the LREE/HREE (**Fig. 4).** *In situ* preferential precipitation of LREE in carbonate-rich environments may occur as HREE-carbonate complexes have higher formation constants. It seems reasonable that a high E:P balance favors carbonate precipitation, and limits the contribution of allocthonous silicates. The higher rainfall during the wet season favors the transport of silicate material into the lake, while higher lake levels (lower E:P values) dilute carbonates and prevent their precipitation. PC1 therefore represents the environmental precipitation balance.

The second principal component positively correlates with TOC and Mo and negatively correlates with the sedimentation rate (**Tab.2**). PC2 decreases between ~3 and ~1 ky BP, and then increase again after 1 ky BP (**Fig.2)**. TOC is associated with primary production both in the water body and its whole basin. The correlation between TOC and Mo may be due to the tendency of Mo to be fixed in the organic components by creating complexes with humic and/or fulvic acids (Gupta, 1997). The low amount of organic matter and the corresponding increase in sedimentation rate between ~3 and ~1 ky BP is also consistent with the well documented Maya Clay Layer (Curtis et al. 1998; Anselmetti et al 2007; Mueller et al. 2009) (**Fig.2**). PC2 represents the erosional processes resulting from increased Mayan agriculture. Erosional processes were more pronounced between ~3 and ~1 ky BP (Anselmetti et al. 2006), but not before ~4.5 ky BP even with increased wet season precipitation. Regional pollen records also depict this land use and vegetation change (Wahl et al. 2007; Fig. 2). Before ~3 ky BP, when the Maya settled in Petén region (Binford 1987), the

vegetation was characterized by tropical forest that prevented erosion even with high rainfall. Erosion was more prevalent during the Pre-Classic and Classic periods, corresponding to agricultural land use and associated reduction of forest cover. This landscape change is clearly associated with anthropogenic activity and corroborated by the presence of *Zea mays* pollen between 3 to ~1 ky (**Fig.2**). The intense drought, that induced the Maya collapse and may have influenced their emigration from the Petén Itzá region, is followed by vegetation similar to pre-Maya conditions, characterized by the recovery of tropical forests (**Fig.2**). Thus, in our view, PC2 represents the anthropogenic impact that is mainly associated with erosional processes and the occurrence of the Maya Clay.

The third component positively correlates with the redox indexes Fe/Mn and V/(V+Ni), and negatively correlates with Mn. Iron and Manganese are strongly affected by the lake's redox conditions. However, Mn is more sensitive than Fe, as Mn precipitate firstly under oxidizing conditions (Davison ,1993; Wetzel, 2001; Dean and Doner, 2012). Increases in Mn correspond to decreases in the other redox indexes (except V/Cr), suggesting that Lake Petén Itzá probably experienced more oxic conditions after ~1 ky BP (**Fig.**). The decrease of PC3 also corresponded to an increase of *Moraceae-Urticaceae* and *Melastomataceae-Combretaceae* pollen and a decrease of *Poaceae* and *Zea mays* pollen suggesting that the change in redox conditions may also be related to the natural response of the biosphere recovering from the anthropogenic impact.

Evidence of the erosion processes and redox conditions were only partially supported by Ce anomaly record (**Fig.4**). As previously discussed, Ce fractionation depends on both preferential leaching and the environmental redox conditions. Ce-complexes are less soluble than other REE-complexes leading to a depletion of the elements while leaching. Along the same lines, Ce^{3+}-complexes are more soluble than the corresponding Ce^{4+}-complexes (Xiong et al. 2012), leading to a Ce enrichment in sediments with respect to the water body in reducing environmental conditions. Although Ce anomalies are not always easy to decipher unambiguously, when leaching processes increase, the preferential dissolution of the other REEs lead to a decrease in Ce/Ce* (**Fig.4)**. A further fractionation could also occur *in situ*, since oxidizing redox conditions favor the formation of the less soluble Ce^{4+} thereby enriching the sediment in Ce and depleting the water body. Thus, sediments become depleted in Ce when non-oxidizing redox conditions occur. However, redox conditions inferred from PC3 and several parameters such as Fe/Mn (Wersin et al. 1991, Naeher et al. 2013) or V/(V+Ni) ratios (Hatch and Leventhal, 1992; Gao et al. 2014) do not completely explain the Ce anomalies. The Ce/Ce* record only partially follows the redox environmental conditions suggested by the other proxies between ~3 and ~1 ky BP. Instead, the Ce/Ce* changes correlate better with TOC than with changing redox conditions. Many authors suggest that Ce anomalies can be affected by the presence of organic matter (Xiong et al 2012 and references therein), although the correlation is only partial. In our record, the Ce/Ce* increase between ~1 and ~1.7 ky BP does not correspond with TOC and the Ce anomaly in Lake Petén Itzá appears to be affected by a combination of both TOC and redox conditions.

The fourth principal component contains several spikes without a clear long-term trend. Nevertheless, the PC4 loadings emphasize the strong correlation between PGEs where these are the same elements with very high enrichment factors, as previously described in the Results section. We hypothesize this extreme enrichment being representative of the PGEs anomaly associated to the Chicxulub Impact Event. Such an anomaly has been detected worldwide in sedimentary facies covering the Kretaceous-Tertiary (K-T) boundary, and is considered as the trace of cosmogenic elements spike originated from the asteroid impact that formed the Chicxulub crater in the Yucatán peninsula (Alvarez et al. 1980, Schute et al 2010; Urrutia-Fucugauchi et al. 2001). The asteroid could have delivered the PGEs to the region, which were then distributed more widely through erosion and associated transport. However, further investigations of PGEs in regional sediments are necessary to determine if PGEs are elevated in sediments throughout the Yucatan peninsula.

The Lake Petén Itzá sediments also demonstrate several spikes of As and Hg that are significantly than the background (**Fig.3).** Regional volcanic eruptions may have caused these

marked increases. This hypothesis is consistent with the volcanic tephra found in the artificial water reserves in Tikal (Tankersley et al 2011) and potentially ascribed to the volcanic activity of Fuego (1380 ± 75 y BP) and Acatenango (2210 ± 275 and 2320 ± 200 y BP). Similarly, eleven eruptive events of El Chichón (1070-1325 y BP, 1320-1445 y BP, 2095-2490 y BP and 1530-2650 y BP) were documented in Tikal (Tankersley et al. 2011). Chemical analysis of the particulate matter of the plume emitted during El Chichón event dated to 1982 A.D., showed a strong enrichment of Hg and As (Kotra et al. 1983), that was more than 3 orders of magnitude higher, when compared with standard volcanic ashes. As shown in **Fig.3**, As and Hg peaks could coincide with these volcanic events. It is also interesting to note that the use of volcanic ashes by Maya civilization in the productions of ceramics was documented (Espindola et al. 2000: Tankersley et al. 2011), although it is not clear if these ashes were collected *in situ* or imported from the highlands through trading routes. However, it seems more likely that the As and Hg spikes can be ascribed to volcanic eruptions rather than a result of ceramic processing.

Conclusions

The Petén Itzá geochemical records for the past 5500 years from core PI 5 VI 02 11B demonstrate that variations in precipitation and agricultural practices altered land-use and associated erosional processes in the Petén Itzá basin. LREE/HREE ratios demonstrate relatively high precipitation rates between ~3 to ~1 ky BP, which agrees with isotopic evidence (Rosenmeier et al 2002; Figs. 2 and 4). This higher precipitation correlates with increased allocthonous silicates in the associated sediments, suggesting intensified erosion during this time period. Our low TOC values between ~3 tand ~1 ky BP are consistent with the low organic content Maya Clay layer containing *Zea Mays* pollen (Wahl et al. 2007; Schüpbach et al. 2015, in **Fig.2** and **Fig.4**). Palinological records demonstrate an absence of *Poaceae* pollen after ~900 yr BP which is ascribed to the termination of large-scale Mayan agriculture due to drought and amplified by anthropogenic land-use (Wahl et al. 2007). Our LREE/HREE, Ce/Ce* values support this major vegetation and land-use change by demonstrating decreased erosion and an increase in TOC. The combination of palynological records with our REE and TE data (**Fig.2** and **Fig.4**) indicate the regrowth of tropical forests after ~1 ky. Once the major Mayan agriculture ended, the regional vegetation reverted to pre-Mayan conditions. Our data demonstrate that the geochemical composition of lake sediments returned to pre-Mayan distributions in coincidence with the decline of Mayan agriculture.

Acknowledgments

This work was financially supported by the Early Human Impact ERC Advance Grant of the European Commission's VII Framework Programme, grant number 267696, contribution no.17. The authors gratefully acknowledge the help of ELGA LabWater in providing the PURELAB Pulse and PURELAB Flex that produced the ultrapure water used in these experiments

REFERENCES

Aide MT and Aide C 2012. Rare Earth Elements: Their Importance in Understanding Soil Genesis, *Soil Science.* **2012**: Article ID 783876, 11 pages. doi:10.5402/2012/783876

Alvarez LW, Alvarez W, Asaro F, Michel HV, 1980. Extraterrestrial cause for the Cretaceous-Tertiary extinction. *Science* **208**: 1095–1108. DOI:10.1126/ science .208 .4448 .1095.

Anselmetti FS, Ariztegui D, Hodell DA, Hillesheim MB, Brenner M., Gilli A, McKenzie JA, Mueller AD, 2006. Late Quaternary climate-induced lake level variations in Lake Petén Itzá, Guatemala, inferred from seismic stratigraphic analysis. *Palaeogeography Palaeoclimatology Palaeoecology* **230**: 52–69.

Anselmetti FS, Hodell DA, Ariztegui D, Brenner M, Rosenmeier MF, 2007.Quantification of soil erosion rates related to ancient Maya deforestation. *Geology* **35**: 915-918. DOI:10.1130/G23834A

Beach T, 1998. Soil constraints on northwest Yucatan, Mexico: pedoarchaeology and Maya subsistence at Chunchucmil. *Geoarchaeology: An International Jornal* **13**: 759-791.

Beach T, Luzzadder-Beach S, Dunning N, Hageman J, Lohse J, 2002. Upland agriculture in the Maya Lowlands: ancient Maya soil conservation in Northwestern Belize. *Geographical Review* **92**: 372-397 DOI:10.1111/j.1931-0846.2002.tb00149.x

Beach T, Dunning N, Luzzadder-Beach S, Cook DE, Lohse J, 2006. Impacts of the ancient Maya on soils and soil erosion in the central Maya Lowlands. *Catena* **65**: 166-178.

Beach T, Luzzadder-Beach S, Dunning N, Cook D, 2008. Human and natural impacts on fluvial and karst depressions of the Maya Lowlands. *Geomorphology* **101**: 308-331.

Beach T, Luzzadder-Beach S, Dunning N, Jones J, Lohse J, Guderjan T, Bozarth S, Millspaugh S, Bhattacharya T, 2009. A review of human and natural changes in Maya Lowlands wetlands over the Holocene. *Quaternary Science Reviews* **28**: 1710-1724.

Beach T, Luzzadder-Beach S, Dunning N, Terry R, Houston S, Garrison T,2011. Carbon isotopic ratios of wetland and terrace soil sequences in the Maya Lowlands of Belize and Guatemala. *Catena* **85**: 109-118.

Beach T, Luzzadder-Beach S, Cook D, Dunning N, Kennett DJ, Krause S, Terry R, Trein D, Valdez F, 2015. Ancient Maya impacts on the Earth's surface: An Early Anthropocene analog?. *Quaternary Science Reviews* **124**: 1-30

Binford MW, Brenner M, Whitmore TJ, Higuera-Gundy A, Deevey ES, Leyden B, 1987. Ecosystems, paleoecology, and human disturbance in subtropical and tropical America. *Quaternary Science Reviews* **6**: 115–128.

Brenner M, 1983. Paleolimnology of the Peten Lake District, Guatemala-II. Mayan population density and sediment and nutrient loading of Lake Quexil. *Hydrobiologia* **103**: 205–210.

Brenner M, Rosenmeier MF, Hodell DA, Curtis JH, 2002. Paleolimnology of the Maya lowlands: long-term perspectives on interactions among climate, environment, and humans. *Ancient Mesoamerica* **13**: 141–157.

Budakoglu M, Abdelnasser A, Karaman M, Kumral M, 2015. The rare earth element geochemistry on surface sediments, shallow cores and lithological units of Lake Acigol basin, Denizli, Turkey. *Journal of Asian Earth Sciences* **111**: 632-662.

Cantrell KJ , Byrne RH, 1987. Rare earth elements complexation by carbonate and oxalate ions. *Geochimica et Cosmochimica Acta* **51:** 597-605

Cook DE, Kovacevich B, Beach T, Bishop R, 2006. Deciphering the inorganic chemical record of ancient human activity using ICP-MS: a reconnaissance study of late Classic soil floors at Cancuén, Guatemala. *Journal of Archaeological Science* **33**: 628-640

Correa-Metrio A, Bush MB, Cabrera KR, Sully S, Brenner M, Hodell DA, Escobar J, Guilderson T, 2012. Rapid climate change and no-analog vegetationin in lowland Central America during the last 86,000 years. *Quaternary Science Reviews* **38**: 63-75.

Curtis JH, Hodell DA, Brenner M. 1996. Climate Variability on the Yucatan Peninsula (Mexico) during the past 3500 Years, and implications for Maya cultural evolution. *Quaternary Research* **46**: 37–47.

Curtis JH, Brenner M, Hodell DA, Balser RA, Islebe GA, Hooghiemstra H, 1998. A multi-proxy study of Holocene environmental change in the Maya Lowlands of Peten, Guatemala. *Journal of Paleolimnology* **19**: 139–159. DOI: 10.1023/A:1007968508262

Dahlin BH, Jensen CT, Terry RE, Wright DR, Beach T, 2007. In search of an ancient Maya market. *Latin American Antiquity* **18**: 363-384 DOI: 10.2307/25478193

Davison W. 1993. Iron and Manganese in lakes. *Earth Science Reviews*. **34**:19-163

Dean WE and Doner LA, 2012. A Holocene record of endogenic iron and manganese precipitation and vegetation history in a lake-fen complex in northwestern Minnesota. *Journal of Palaeolimnology*. **47**: 29-42.

Deevey ES, Brenner M, Flannery MS, Yezdani GH, 1980: Lakes Yaxha and Sacnab, Petén, Guatemala: limnology and hydrology. Arch. Hydrobiol. 57, 419-460.

Diamond J, 2005. Collapse: How societies choose to fail or succeed, New York, Viking

Eberl M, Alvarez M, Terry RE, 2012. Chemical Signatures of middens at a late classic maya residential complex, Guatemala **27**: 426–440 DOI: 10.1002/gea.21415

Espindola JM et al. 2000. Volcanic history of El Chichon volcano (Chiapas, Mexico) during the Holocene and its impact on human activity. Bulletin of Volcanology 62: 90-104

Gao C, Bao K, Lin Q, Zhao H, Zhang Z, Xing W, Lu X, Wang G, 2014. Characterizing trace and major elemental distribution in the late Holocene in Sanjiang Plain, Notheast China: Paleoenvironmental implication. *Quaternary International* **349**: 376-383.

Gill RB, 2000. The great Maya droughts: water, life, and death. *Albuquerque: University of New Mexico Press* **44**: 216-218

Gromet LP, Haskin LA, Korotev RL, Dymek RF, 1984. The "North American Shale Composite": its compilation, major and trace element characteristics. *Geochimica et Cosmochimica Acta* **48**: 2469-2482.

Gupta UC 1997. Molybdenum in agriculture. *Cambridge University Press*

Haskin LA, Wildeman TR, Frey FA, Collins KA, Keedy CR, Haskin MA, 1966. Rare earths in sediments. *Journal of geophysical Research* **71**: 6091–6105. DOI: 10.1029/JZ071i024p06091

Hatch JR, Leventhal JS, 1992. Relationship between inferred redox potential of the depositional environment and geochemistry of the Upper Pennsylvanian (Missourian) Stark Shale Member of the Dennis Limestone, Wabaunsee County, Kansas, USA. *Chemical Geology* **99**: 65-82.

Haug GH, Gunter D, Peterson LC, Sigman DM, Hughen KA, Aeschlimann B, 2003. Climate and the collapse of Maya civilization. *Science* **299**: 1731-1735 DOI: 10.1126/science.1080444

Hillesheim MB, Hodell DA, Leyden BW, Brenner M, Curtis JH, Anselmetti FS, Ariztegui D, Buck DG, Guilderson TP, Rosenmeier MF, Schnurrenberger DW, 2005. Climate change in lowland Central America during the late deglacial and early Holocene. *Journal of Quaternary Science* **20**: 363–376. DOI: 10.1002/jqs.924

Hodell DA, Brenner M, Curtis JH, 2000. Climate change in the northern American tropics since the last Ice Age: implications for environment and culture. In: Lentz DL (Rds), Imperfect Balance: Landscape transformations in the Precolumbian Americas. Columbia University Press, New York, pp. 13-38

Hodell DA, Anselmetti FS, Ariztegui D, Brenner M, Curtis JH, Gilli A, Grzesik DA, Guilderson TJ, Muller AD, Bush MB, Correa-Metrio A, Escobar J, Kutterolf S, 2008. An 85-ka record of climate change in lowland Central America. *Quaternary Science Reviews* **27**: 1152–1165.

Hosler WT, 1997. Evaluation of the application of rare-earth elements to the paleoceanogrphy. *Palaeoceanography, Palaeoclimatology, Palaeoecology* **132**: 309-323

Hutson SR, Terry RE, 2006: Recovering social and cultural dynamics from plaster floors: chemical analyses at ancient Chunchucmil, Yucatan, Mexico. *Journal of Archaeological Science* **33** : 391-404

Islebe GA, Hooghiemstra H, Brenner M, Curtis JH, Hodell DA,1996. A Holocene vegetation history from lowland Guatemala. *The Holocene* **6**

Jones B, Manning DAC, 1994. Comparison of geochemical indices used for the interpretation of palaeoredox conditions in ancient mudstones. *Chemical Geology* **111**: 111-129.

Kennett DJ, Breitenbach SFM, Aquino VV, Asmerom Y, Awe J, Baldini JUL, Bartlein P, Culleton BJ, Ebert C, Jazwa C, Macri MJ, Marwan N, Polyak V, Prufer KM, Ridley HE, Sodemann H, Winterhalder B, Haug GH, 2012. Development and disintegration of Maya political systems in response to climate change. *Science* **338**: 788-791. DOI: 10.1126/science1226299

Kidder DL, Krishnaswamy R, Mapes RH 2003. Elemental mobility in phosphatic shales during concretion growth and implications for provenance analysis. Chemical geology 198: 335-353

Kotra JP et al 1983 El Chichon: Composition of Plume Gases and Particles. Science 222:1018-1021

Kotto-Same J, Woomer PL, Appolinaire M, Louis Z, 1997. Carbon dynamics in slash-and-burn agriculture and land use alternatives of the humid forest zone in Cameroon. *Agriculture, Ecosystems and Environment* **65**: 245-256

Lee JH, Byrne RH, 1993. Complexation of trivalent rare earth elements (Ce, Eu, Gd, Tb, Yb) by carbonate ions. *Geochimica et Cosmochimica Acta* **57**: 295-302

Leyden BW, 2002: Pollen evidence for climatic variability and cultural disturbance in the Maya Lowlands. *Ancient Mesoamerica* **13**: 85-101

Lewis SL, Maslin MA, 2015. Defining the Anthropocene. *Nature* **519**: 171-180 DOI: 10.1038/nature14258

Luo YR and Byrne RH, 2004. Carbonate complexation of yttrium and rare earth elements in natural waters, Geochimica et Cosmochimica Acta. 68: 691-699.

Luzzadder-Beach S, Beach T ,2009. Arising from the wetlands, mechanism and chronology of landscape aggradation in the northern coastal plain of Belize. *Annals of the Association of American Geographers* **99**: 1-26

Luzzadder-Beach S, Beach T, Terry RE, Doctor KZ, 2011. Elemental prospecting and geoarchaeology in Turkey and Mexico. *Catena* **85**: 119-129.

Middleton WD, 2004. Identifying chemical activity residues on prehistoric house floors: A methodology and rationale for multi-elemental characterization of a mild acid extract of anthropogenic sediment. *Archaeometry* **46**: 47–65. DOI: 10.1111/j.1475-4754.2004.00143.x

Mueller AD, Islebe GA, Hillesheim MB, Grzesik DA, Anselmetti FS, Aritzegui D, Brenner M, Curtis JH, Hodell DA, Venz KA 2009. Climate drying and associated forest decline in the lowlands of northern Guatemala during the late Holocene. *Quaternary Research* **71**: 133-141.

Murray RW, Buchholtz ten Brink MR, Brumsack HJ, Gerlach DC, Russ III GP, 1991: rare earth elements in Japan sea sediment and diagenetic behavior of Ce/Ce*: results from ODP Leg 127. Geochimica et Cosmochimica Acta 55:2453-2466

Naeher S, Gilli A, North RP, Hamann Y, Schubert CJ, 2013. Tracing bottom water oxygenation with sedimentary Mn/Fe ratios in Lake Zurich, Switzerland.

Och LM, Muller B, Wichser A, Ulrich A, Vologina EG, Sturm M, 2014. Rare earth elements in the sediments of Lake Baikal. *Chemical Geology* **376**: 61-75.

Parnel JJ, Terry RE, Zachary N, 2002. Soil Chemical Analysis Applied as an Interpretive Tool for Ancient Human Activities in Piedras Negras, Guatemala. *Journal of Archaeological Science* **29**: 379–404

Peterson LC, Haug GH, 2005. Climate and the collapse of Maya civilization. *American Scientist* **93**: 322-329

Pourret O, Davranche M, Gruau G, Dia A, 2007. Competition between humic acid and carbonates for are earth elements complexation. Journal of Colloid and Interface Science. 305: 25-31.

Reimann C, De Caritat P, 2000. Intrinsic Flaws of Element Enrichment factors (EFs) in environmental geochemistry. *Environmental Science and Tecnology* **34**: 5084-5091 DOI: 10.1021/es001339o

Rice DS, Rice PM, 1990. Population size and population change in the Central Peten Lake Region Guatemala. In Culbert Rice (eds) Precolumbian population history in the Maya Lowlands. *Albuquerque, New Mexico, University of New Mexico Press* 123–148.

Rosenmeier MF, Hodell DA, Brenner M, Curtis JH, Martin JB, Anselmetti FS, Aritzegui D, Guilderson TP, 2002. Influence of the vegetation change on watershed hydrology: implications for paleoclimatic interpretation of lacustrine $\delta^{18}O$ records. *Journal of Paleolimnology* **27**: 117-131 DOI: 10.1023/A:1013535930777

Royston P, 1992. Approximating the Shapiro-Wilk-W-test for non-normality. *Statistics and Computing* **2**: 117-119. DOI: 10.1007/BF01891203

Rudnick RL, Gao S, 2003. Composition of the Continental Crust. *In Treatise on Geochemistry* **3**: 1-64 DOI: 10.1016/B0-08-043751-6/03016-4

Scarborough VL, 1993: Water management in the southern Maya Lowlands: an accretive model for the engineered landscape. In: scarborough VL, Isaac B (eds) Economic Aspects of water management in the prehispanic new world. Research in Economic Anthropoloy Supplement 7 JAI, Greenwich, CT. pp. 17-68

Schupbach S, Kirchgeorg T, Colombaroli D, Beffa G, Radaelli M, Kehrwald NM, Barbante C, 2015. Combining charcoal sediment and molecular markers to infer a Holocene fire history in the Maya Lowlands of Peten, Guatemala. *Quaternary Science reviews* **115**: 123-131.

Shapiro SS, Wilk MB, 1965. An analysis of variance test for normality (complete samples). *Biometrika* **52** 591-611.

Schulte P, Alegret L, Arenillas I, Arz JA, Barton PJ, Bown PJ, Bralower TJ, Christeson GL, Goto K, Grajales-Nishimura JM, Grieve RAF, Gulick SPS, Jhonson KR, Kiessling W, Koeberl C, Kring DA, MacLeod KG, Matsui T, Melosh J, Montanari A, Morgan JV, Neal CR, Nichols DJ, Norris RD, Pierazzo E, Ravizza G, Sweet AR, Urrutia-Fucugauchi J, Vajda V, Whalen MT, Willumsen PS, 2010. The Chicxulub Asteroid Impact and Mass Extinction at the Cretaceous-Paleogene Boundary. *Science* **327:** 1214-1218 DOI: 10.1126/science.1177265

Tankersley KB et al 2011. Evidence for volcanic ash fall in the Maya Lowlands from a reservoir at Tika, Guatemala, Journal of Archaeological Science 38. 133-143

Taylor SR, McLennan SM 1985. The Continental Crust: Its Composition and Evolution. *SciTech Connect*

Tribovillard N, Algeo TJ, Lyons T, Riboulleau A, 2006. Trace metals as paleoredox and paleoproductivity proxies: An update. *Chemical Geology* **232**: 12-32.

Urrutia-Fucugauchi J, Camargo-Zanoguera A, Pérez-Cruz L, 2011. Discovery and focused study of the Chicxulub impact crater. *EOS* **92**: 209–210 DOI: 10.1029/2011EO250001

Vaughan HH, Deevey ES, Garrett-Jones SE, 1985. Pollen stratigraphy of two cores from the Petén lake district, with an appendix on two deep-water cores. In Pohl M (eds), Prehistoric Lowland Maya Environment and Subsistence Economy. Harvard University Press, Cambridge, 73-89

Wahl D, Byrne R, Schreiner T, Hansen R 2007. Palaeolimnological evidence of late-Holocene settlements and abandonment in the Mirador Basin, Peten, Guatemala, *The Holocene* **6**: 813-820

Wahl D, Byrne R, Schreiner T, Hansen R 2006, Holocene vegetation change in the northern Petén and its application for Maya Prehistory. Quaternary research 65:380-389.

Wang J, Zhu L, Wang Y, Gao S, Daut G, 2012. A comparison of different methods for determining the organic and inorganic carbon content of lake sediments from two lakes on the Tibetan Plateau. Quaternary International 205: 49-54

Wells EC, Terry RE, Parnell JJ, Hardin PJ, Jackson MW, Houston SD, 2000. Chemical Analyses of Ancient Anthrosols in Residential Areas at Piedras Negras, *Guatemala Journal of Archaeological Science* **27**: 449–462

Wen XY, Huang CM, Tang Y, Gong-Bo SL, Hu XX, Wang ZW, 2014. Rare earths elements: a potential proxy for identifying the lacustrine sediment source and soil erosion intensity in karst areas. *Journal of Soils and Sediments* **14*:*** 1693-1702. DOI: 10.1007/s11368-014-0928

Wersin P, Höhener P, Giovanoli R, Stumm W, 1991. Early diagenetic influences on iron transformations in a freshwater lake sediment. *Chemical Geology* **90**: 233-252.

Wetzel RG 2001. Limnology: lake and river ecosystems, 3rd edn. Academic Press, San Diego

Whitmore TJ, Brenner M, Curtis JH, Dahlin HB, Leyden BW. 1996. Holocene Climate and Human Influences on Lakes of the Yucata´n Peninsula, Mexico: An Interdisciplinary Palaeolimnological Approach. *The Holocene* **6**: 273–287

Xiong Z, Li T, Algeo T, Chang F, Yin X, Xu Z, 2012. Rare earth element geochemistry of laminated diatom mats from tropical West Pacific: Evidence for more reducing bottomwaters and higher primary productivity during the Last Glacial Maximum. *Chemical Geology* **296**: 103-118

Table 1. Statistical parameters of elemental concentration distributions and results for the Shapiro-Wilk normality test (H_0) (Shapiro and Wilk, 1965; Royston et al. 1992).

	Minimum	Maximum	Max/Min	Mean	SD	W-Coefficient	*p*-Value	Accept H_0
Al (mg g^{-1})	29.4	76.7	2.61	48.9	9.5	0.9796	0.4730	Yes
V (µg g^{-1})	44.6	92.8	2.08	63.7	11.2	0.9697	0.1777	Yes
Cr (µg g^{-1})	16.5	38.7	2.35	25.7	4.8	0.9791	0.4514	Yes
Mn (µg g^{-1})	181	604	3.34	370	121	0.9540	0.0365	Yes
Fe (mg g^{-1})	13.6	30.7	2.26	21.4	3.9	0.9766	0.3568	Yes
Co (µg g^{-1})	4.0	8.2	2.05	6.1	1.0	0.9746	0.2963	Yes
Ni (µg g^{-1})	14.7	28.2	1.90	20.0	3.2	0.9672	0.1375	Yes
Cu (µg g^{-1})	16.4	38.6	2.35	24.5	4.9	0.9464	0.0162	Yes
Zn (µg g^{-1})	*39.8*	*104.8*	*2.65*	*59.2*	*12.1*	*0.9356*	*0.0056*	*No*
As (µg g^{-1})	*4.5*	*15.6*	*3.48*	*7.05*	*1.82*	*0.8453*	*0.0000*	*No*
Sr (µg g^{-1})	209	383	1.83	277	47	0.9513	0.0264	Yes
Mo (µg g^{-1})	*0.61*	*2.03*	*3.34*	*1.11*	*0.39*	*0.9247*	*0.0020*	*No*
Ag (ng g^{-1})	*207*	*552*	*2.66*	*372*	*99*	*0.9339*	*0.0048*	*No*
Cd (ng g^{-1})	*391*	*992*	*2.54*	*550*	*145*	*0.8730*	*0.0000*	*No*
Sn (µg g^{-1})	*0.38*	*2.60*	*6.84*	*0.83*	*0.36*	*0.8274*	*0.0000*	*No*
Sb (µg g^{-1})	0.53	1.37	2.59	0.90	0.20	0.9664	0.1262	Yes
Ir (ng g^{-1})	*3.1*	*10.3*	*3.32*	*5.0*	*1.5*	*0.9186*	*0.0012*	*No*
Pt (ng g^{-1})	*8.7*	*29.3*	*3.36*	*14.7*	*4.3*	*0.9167*	*0.0011*	*No*
Au (ng g^{-1})	*1.1*	*14.9*	*13.08*	*4.1*	*2.2*	*0.8163*	*0.0000*	*No*
Hg (ng g^{-1})	*32*	*112*	*3.47*	*52*	*14*	*0.8205*	*0.0000*	*No*
Pb (µg g^{-1})	7.6	17.7	2.33	11.0	2.0	0.9660	0.1207	Yes
Bi (ng g^{-1})	116	306	2.64	193	41	0.9791	0.4509	Yes
U (µg g^{-1})	1.8	3.5	1.94	2.45	0.43	0.9601	0.0656	Yes
Ce (µg g^{-1})	22.8	53.9	2.36	35.2	7.9	0.9622	0.0811	Yes
ΣREE* (µg g^{-1})	33.2	78.8	2.38	53.7	11.3	0.9660	0.1209	Yes

Table 2. Loadings of the investigated elements in the first four principal components obtained by PCA analysis of the entire dataset. High and moderate loadings are marked in bold text.

	PC1	**PC2**	**PC3**	**PC4**
Eigenvalue	19.69	4.69	1.61	1.23
% Variance	63.5	15.1	5.2	4.0
Cumulative	63.5	78.7	83.8	87.8
Al	**0.848**	-0.315	0.075	0.286
V	**0.666**	0.466	0.349	0.427
Cr	**0.865**	-0.018	0.289	0.358
Mn	-0.393	-0.300	**-0.725**	-0.318
Fe	**0.847**	-0.007	0.343	0.366
Co	**0.729**	0.527	-0.161	0.289
Ni	0.644	**0.630**	0.102	0.364
Cu	0.551	**0.672**	0.237	0.387
Zn	**0.692**	0.298	0.171	0.554
As	0.528	-0.386	-0.242	0.269
Sr	**-0.690**	-0.217	-0.573	-0.156
Mo	0.338	**0.861**	-0.017	0.144
Ag	**0.783**	0.192	0.376	0.393
Cd	0.364	**0.749**	0.196	0.470
Sn	0.556	0.242	0.164	**0.655**
Sb	**0.763**	0.112	0.243	0.523
Ir	0.392	0.259	0.195	**0.785**
Pt	0.374	0.303	0.216	**0.804**
Au	0.205	0.232	0.181	**0.747**
Hg	**0.724**	0.019	-0.057	-0.020
Pb	**0.675**	0.374	0.109	0.588
Bi	**0.745**	0.223	0.246	0.539
U	0.580	0.542	0.269	0.481
Ce	**0.691**	0.401	0.183	0.513
ΣREE*	**0.788**	0.178	0.148	0.510
Fe/Mn	0.530	0.342	**0.617**	0.373
V/(V+Ni)	0.228	-0.312	**0.718**	0.244
V/Cr	-0.463	**0.777**	0.090	0.079
TIC	**-0.816**	-0.196	-0.372	-0.024
TOC	0.144	**0.935**	-0.065	0.125
Sedimentation rate	0.190	**-0.899**	-0.165	-0.184

Table 3 Enrichment Factors calculated using the equation (1) and Earth's crust (Rudnik and Gao 2014) or Average Shale ([a]=Taylor 2010; [b]=Tribovillard et al. 2006) and North American Shale Composite (NASC, [c]=Haskin et al 1966) as the reference. n.a.= reference not available. Uncertainty was considered as the corresponding SD

Element	Enrichment Factor (Crustal)	Enrichment Factor (Shale)
V	1.11 (±0.18)	0.97 (±0.15)[a]
Cr	0.47 (±0.04)	0.55 (±0.05)[a]
Mn	0.85 (±0.40)	0.98 (±0.45)[a]
Fe	1.02 (±0.10)	0.89 (±0.09)[a]
Co	0.59 (±0.09)	0.65 (±0.10)[a]
Ni	0.72 (±0.12)	0.86 (±0.15)[a]
Cu	1.49 (±0.30)	0.88 (±0.18)[a]
Zn	1.49 (±0.24)	1.48 (±0.24)[a]
As	2.47 (±0.50)	0.53 (±0.10)[c]
Sr	1.53 (±0.55)	3.11 (±1.11)[a]
Mo	1.72 (±0.60)	2.40 (±0.84)[c]
Ag	11.70 (±2.22)	n.a.
Cd	10.45 (±2.82)	3.96 (±1.07)[c]
Sn	0.65 (±0.23)	0.29 (±0.10)[b]
Sb	3.75 (±0.52)	0.91 (±0.13)[c]
Ir	**385.7 (±96.4)**	**n.a.**
Pt	**49.7 (±12.9)**	**n.a.**
Au	4.54 (±2.27)	n.a.
Hg	1.75 (±0.38)	n.a.
Pb	1.09 (±0.21)	1.17 (±0.22)[a]
Bi	2.03 (±0.28)	1.64 (±0.23)[a]
U	1.55 (±0.28)	1.70 (±0.30)[a]
ΣREE*	1.02 (±0.15)	1.02 (±0.15)[a]

Table 4. Maximum, minimum, mean and standard deviation of Rare Earth Elements (REEs) concentration.

	Minimum	**Maximum**	**Mean**	**SD**	**REE**
La(μg g^{-1})	11.5	27.0	18.0	3.7	LREE
Ce(μg g^{-1})	22.8	53.9	35.2	7.9	
Pr(μg g^{-1})	2.6	6.4	4.3	0.9	
Nd(μg g^{-1})	10.2	24.5	16.5	3.5	
Sm(μg g^{-1})	1.98	4.79	3.28	0.70	MREE
Eu(μg g^{-1})	0.48	1.10	0.75	0.15	
Gd(μg g^{-1})	1.98	4.76	3.23	0.68	
Tb(μg g^{-1})	0.28	0.72	0.48	0.10	
Dy(μg g^{-1})	1.62	4.24	2.77	0.62	
Ho(μg g^{-1})	0.32	0.86	0.56	0.13	
Er(μg g^{-1})	0.96	2.60	1.69	0.39	HREE
Tm(μg g^{-1})	0.14	0.38	0.25	0.06	
Yb(μg g^{-1})	0.92	2.69	1.70	0.42	
Lu(μg g^{-1})	0.14	0.41	0.26	0.06	
ΣREE	55.9	132.3	88.7	19.0	

Fig.1


El Chichon
100 km
Tikal
Lake Petén Itzà
Salpetén
Fuego
Acatenango
Mérida
Cancun
Playa del Carmen
Tulum
YUCATAN
Campeche
CAMPECHE
QUINTANA ROO
Ciudad del Carmen
Chetumal
Villahermosa
CHIAPAS
Belmopan
Belize
Tuxtla Gutiérrez
Guatemala
La Ceiba
Tapachula
Città del Guatemala
San Pedro Sula
Honduras
Antigua Guatemala
Tegucigalpa
El Salvador
Tikal
Lake Petén Itzà
Salpetén
10 km

Fig.2

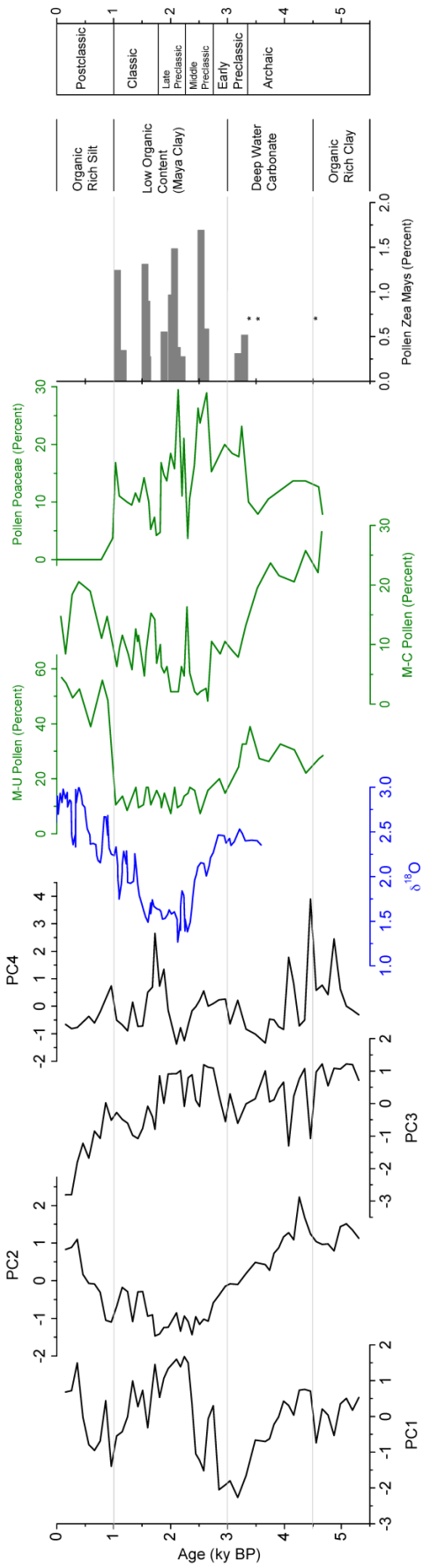
Postclassic
Classic
Late Preclassic
Middle Preclassic
Early Preclassic
Archaic
Organic Rich Silt
Low Organic Content (Maya Clay)
Deep Water Carbonate
Organic Rich Clay
Pollen Zea Mays (Percent)
Pollen Poaceae (Percent)
M-U Pollen (Percent)
M-C Pollen (Percent)
δ18O
PC4
PC3
PC2
PC1
Age (ky BP)

Fig.3

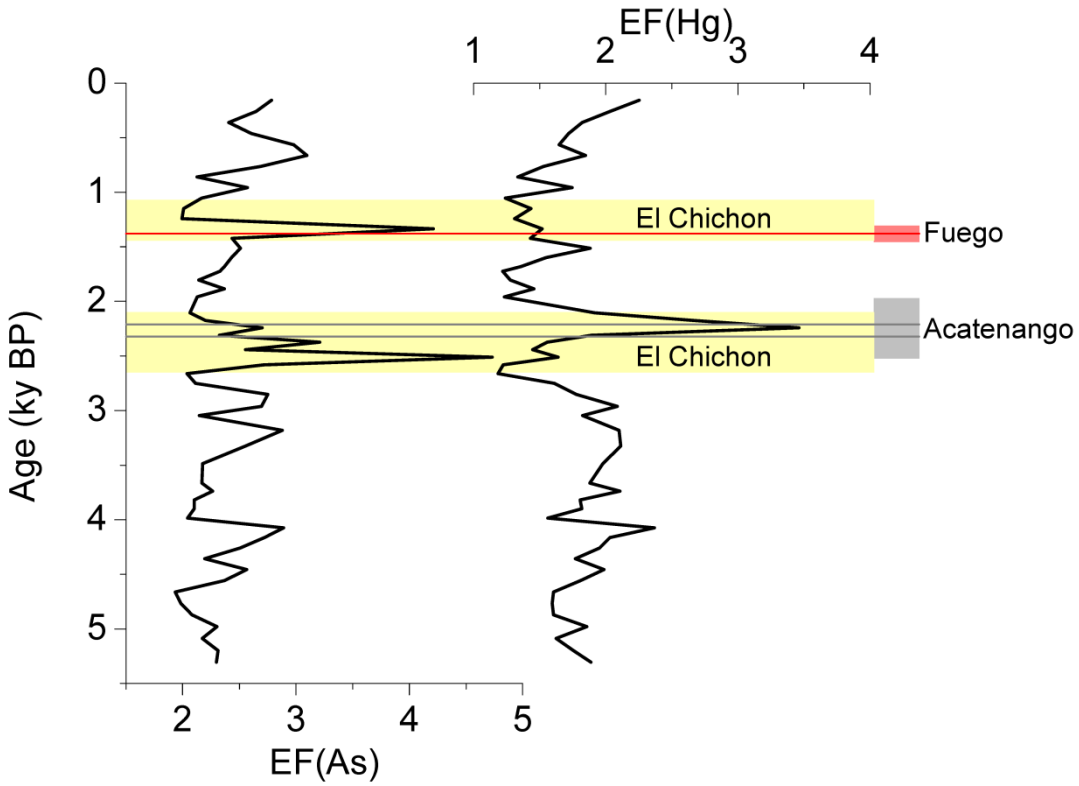
EF(Hg)
1
2
3
4
0
1
2
3
4
5
Age (ky BP)
El Chichon
Fuego
Acatenango
El Chichon
2
3
4
5
EF(As)

Fig.4

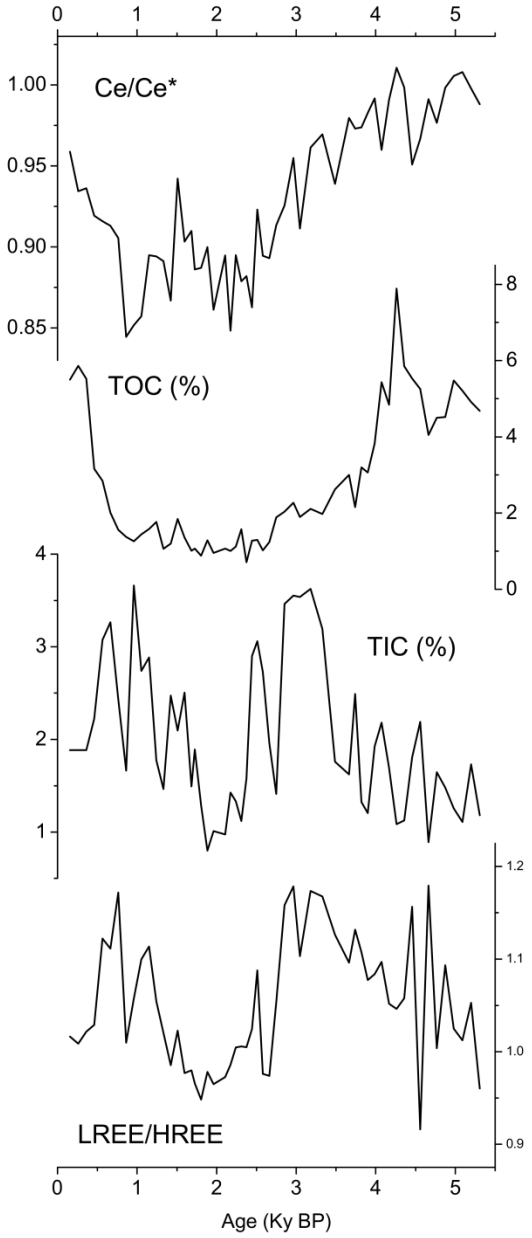

Figure Captions

Fig.1 Map of the Yucatán region, showing the study site at Lake Petén Itzá, Lake Salpetén, Tikal and the main volcanoes mentioned in this study.

Fig.2 Factor Scores of PC1-PC4, compared to $\delta^{18}O$ in Lake Salpetén (Rosenmeier et al. 2002) and Petén pollen records (Wahl et al. 2006) (M-U=*Moraceae-Urticaceae*; M-C= *Melastomataceae-Combretaceae*). Lithologic and lithostratigraphic units are described in detail in (Hillesheim et al 2005 and Mueller et al 2009).

Fig.3 Temporal variability in As and Hg Enrichment Factors and major documented volcanic events (Espindola et al. 2000; Tankersley et al. 2011)

Fig.4 Comparison between Ce/Ce* and LREE/HREE record with TOC% (from Schüpbach et al 2015) and TIC% in Lake Petén Itza sediments.

Supporting Material

Table 1S. Analytical performance of the method employed in this study (a) evaluated using the certified estuarine sediment (BCR-667) as a reference.

Element	LOD_{met} (µg g^{-1})	Recovery (%)[a]	RSD (%)[a]
Al	0.08	-	11
V	0.008	-	4
Cr	0.01	92±14	11
Mn	0.005	89±7	4
Fe	0.2	91±5	6
Co	0.0008	89±9	3
Ni	0.003	91±11	4
Cu	0.02	94±18	5
Zn	0.2	107±12	5
As	0.009	130±23	4
Sr	0.009	101±10	3
Mo	0.0005	-	4
Ag	0.0002	-	7
Cd	0.002	108±23	2
Sn	0.5	-	3
Sb	0.001	111±11	2
La	0.003	96±6	4
Ce	0.008	91±5	7
Pr	0.001	103±13	5
Nd	0.003	97±8	3
Sm	0.002	104±8	4
Eu	0.0004	104±9	3
Gd	0.0001	107±6	1
Tb	0.0003	100±6	3
Dy	0.0006	95±7	3
Ho	0.0001	92±10	3
Er	0.0002	91±9	3
Tm	0.0001	91±11	3
Yb	0.0005	90±8	3
Lu	0.0002	89±9	4
Hg	0.002	-	5
Ir	0.002	-	15
Pt	0.002	-	12
Au	0.0008	81±13	8
Pb	0.004	110±9	4
Bi	0.0005	-	3
U	0.0002	114±13	5